

## Mn-Zn Ferrite Prepared by Sr<sup>2+</sup> Doping

Neng-Wei WANG<sup>1,a,\*</sup>, Shao-Xia XIA<sup>2,b</sup> and You LI<sup>3,c</sup>

School of Material Science and Engineering, Panzhihua University, 617000 Panzhihua,  
Sichuan Province, People's Republic of China.

<sup>a</sup> wnw\_2008@163.com, <sup>b</sup> 1442193054@qq.com, <sup>c</sup> 895102533@qq.com.

**Keywords:** Sol-gel, Sr<sup>2+</sup> Doping, Sintered, Morphologies, TGA.

**Abstract.** In this paper, the effect of different concentration of Sr<sup>2+</sup> doping on the synthesis of Mn-Zn ferrite precursor by sol-gel method was studied, and the final product was synthesized by high temperature sintering. It showed that the spinel phase ZnFe<sub>2</sub>O<sub>4</sub> of Mn-Zn ferrite gradually increased with the increase of the sintering temperature by X-ray Diffraction (XRD) analysis, and at last almost the entire ZnFe<sub>2</sub>O<sub>4</sub> phase was obtained. The grain size and the aggregation state were effected directly by the sintering temperature by Scanning Electron Microscope (SEM) analysis. The obvious change of grain size and the phenomenon of agglomeration were observed with the increase of the sintering temperature. It also showed that the precursor reacted violently at the temperature of 225-227°C by thermal analysis. With the increase of the content of strontium, the reaction time was greatly shortened, and the new phase of the formation was also generated more.

### Introduction

In the basic point of view of magnetism, all the material in the world is magnetic. Magnetic material industry, as a basic material industry, relates to electronic information, mechanical and electrical, automotive, metallurgy, mining, aerospace, transportation, biomedical and other industrial sectors and public utilities sector [1-5]. At present, magnetic material is only a kind of functional material, which is only used in the field of high technology and traditional technology after semiconductor material is applied in that.

In early 1930s, the Holland scientists were represented by Snooker who found some large strong magnetic materials. They are used in high frequency AC conditions with good performance, which is known as the ferrite. Ferrite is a kind of oxide magnetic material, which has both strong magnetic properties and high resistivity [6-9]. With the rapid development of ferrite in computer technology and communication technology, it has greatly promoted the rapid development of all electronic technology.

Mn-Zn ferrite is a typical representative of soft magnetic material. It has many advantages, such as high permeability, high saturation magnetization, low coercive force, low loss, etc. It has been widely used in IT industry, aviation and aerospace, transportation and national defense weapon system and other departments of the national economy and the people's livelihood, its output occupies more than 60% of the total output of soft ferrite materials.

Mn-Zn ferrite is cubic spinel type ferrite, the space group is F3dm, the chemical formula can be expressed by XFe<sub>2</sub>O<sub>4</sub>, in which the X is expressed with two valence ions Fe<sup>2+</sup> similar metal ions, such as: Mg<sup>2+</sup>, Zn<sup>2+</sup>, Co<sup>2+</sup>, Mn<sup>2+</sup> and other metal ions [10-13]. Fe<sup>3+</sup>, Al<sup>3+</sup>, Ti<sup>4+</sup>, Cr<sup>3+</sup> and so on plasma exchange. The principle that they can be exchanged is that the sum of the total chemical valence between a numbers of metal ions is 8 and can be balanced with the chemical valence of the 4 cations. A unit cell of the spinel type crystal structure has a total of 56 ions, which is equivalent to 8 XFe<sub>2</sub>O<sub>4</sub>. There are 32 oxygen ions in the unit cell. The metal ions have a total of 24, each unit cell can be divided into 8 small cubes. They are equally divided into two types: the same type are two common edges of small cubes; different types are two coplanar small cubes.

To increase the magnetic performance of the Mn-Zn ferrite, chemical composition of the doping is a very important way. The doping of Mn-Zn ferrite can be divided into the doping of the lattice of the ferrite and the doping of the undoped lattice, however, the ions into the lattice can be divided

into two categories: interstitial impurity atom and substitutional impurity ion. Thereinto, if the foreign ion's radius is a little small, it would enter easily the lattice. When the impurity radius is not big, it is easy to be replaced, then the magnetic properties of ferrite is ameliorated.

## Experiments

### Test sample Preparation

In the experiment, the Mn-Zn ferrite precursor was prepared by sol-gel method, and the final product was synthesized by high temperature sintering. The experimental flow chart was shown in figure 2.1. In the preparation of Mn-Zn ferrite precursor, some raw materials were used including manganous nitrate  $[\text{Mn}(\text{NO}_3)_2 \cdot 4\text{H}_2\text{O}]$  (solution, the mass fraction of 50%) 21.5mol%, zinc nitrate  $[\text{Zn}(\text{NO}_3)_2 \cdot 6\text{H}_2\text{O}]$  11.5mol%, iron nitrate  $[\text{Fe}(\text{NO}_3)_3 \cdot 9\text{H}_2\text{O}]$  67mol% , concentrated ammonia  $[\text{NH}_4\text{OH}]$  and citric acid  $[\text{C}_6\text{H}_8\text{O}_7 \cdot 6\text{H}_2\text{O}]$ . Concentrated ammonia  $[\text{NH}_4\text{OH}]$  was used as alkaline solution to adjust pH value, citric acid  $[\text{C}_6\text{H}_8\text{O}_7 \cdot 6\text{H}_2\text{O}]$  was used as complexing agent, which of the total content was equal to the total metal ion.  $\text{Sr}^{2+}$  was provided for metal ion doping by  $\text{Sr}(\text{NO}_3)_2 \cdot 9\text{H}_2\text{O}$ ,  $x=0, 0.1, 0.2, 0.3\text{mol}\%$ . The ingredients were dissolved in about 350mL of deionized water, stirring until completely dissolved. The pH value was adjusted to 5.0 by ammonia, then adjustment was stopped. The solution was poured into a water bath to heat, the temperature was set to  $80^\circ\text{C}$ , stirring by strong stirrer, until it became reddish brown of the sol. At room temperature, the sol was placed for 2 hours, the gel was obtained, and the gel was then dried in the oven, the temperature was set at  $110^\circ\text{C}$ . Dried gel was ground into powder in agate mortar. It was calcined at  $900^\circ\text{C}$  and  $1200^\circ\text{C}$  for 3h respectively. The final powder was obtained by grinding for the calcined product.

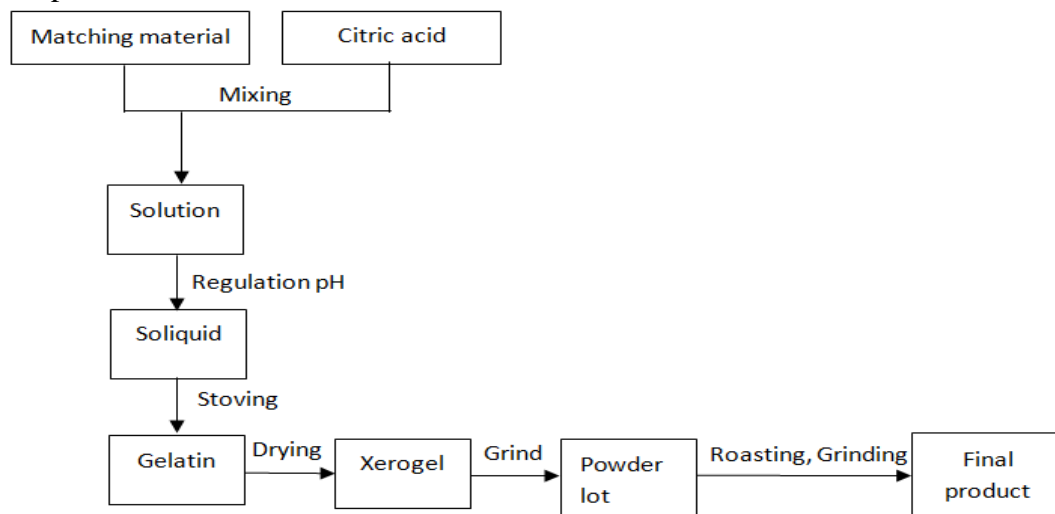


Figure 2.1 Experimental flow chart

### Experimental Sample Tested

The precursor's exothermic and endothermic was tested by the Thermo Gravimetric Analyzer (TGA) in the experiment. The powders' pattern was observed by Scanning Electron Microscope (SEM). Phase change of the powder was analyzed by X-ray Diffraction (XRD).

## Analysis and Discussion

### Analysis of XRD

The samples for different contents of  $\text{Sr}^{2+}$  doping and different sintering temperature were analyzed

by XRD, the composition of the product would be determined. The selected scanning angle was between  $20^\circ$  and  $65^\circ$  in the experiment. Pure Cu was used as target,  $\lambda=1.5406\text{\AA}$ . X diffraction patterns were given with different content of  $\text{Sr}^{2+}$  doping and sintered at  $900^\circ\text{C}$  (see Figure 3.1(a)). Compared with the standard PDF card, spinel type  $\text{ZnFe}_2\text{O}_4$  product is determined according to the three peak, corresponding angles  $2\theta$  are  $35.3^\circ$ ,  $29.9^\circ$  and  $62.2^\circ$  respectively. Meanwhile paramagnetic impurity  $\alpha\text{-Fe}_2\text{O}_3$  is also found out according to the other three peak, corresponding angles  $2\theta$  are  $33.2^\circ$ ,  $35.7^\circ$ ,  $54.1^\circ$ . After the powder was calcined at  $1200^\circ\text{C}$  for 3h, paramagnetic impurity  $\alpha\text{-Fe}_2\text{O}_3$  almost disappeared, nearly all the products were  $\text{ZnFe}_2\text{O}_4$ . which were analyzed by XRD (see Figure 3.1(b)). It was discovered that  $2\theta$  reached  $35.20^\circ$  ( $\text{Sr}^{2+}=0.1$ ),  $35.09^\circ$  ( $\text{Sr}^{2+}=0.2$ ),  $34.98^\circ$  ( $\text{Sr}^{2+}=0.3$ ) from  $35.22^\circ$  ( $\text{Sr}^{2+}=0$ ) by analysis of the angle of the main crystal plane (311), respectively, in other words, the main crystal surface deviated generally to a small angle. Furthermore, the more the amount of dopant was, the more obvious the deviation was. It is mainly due to the amount of  $\text{Sr}^{2+}$  doping, which increases the lattice constant. It indicated that  $\text{Sr}^{2+}$  doping reached the expectant effect.

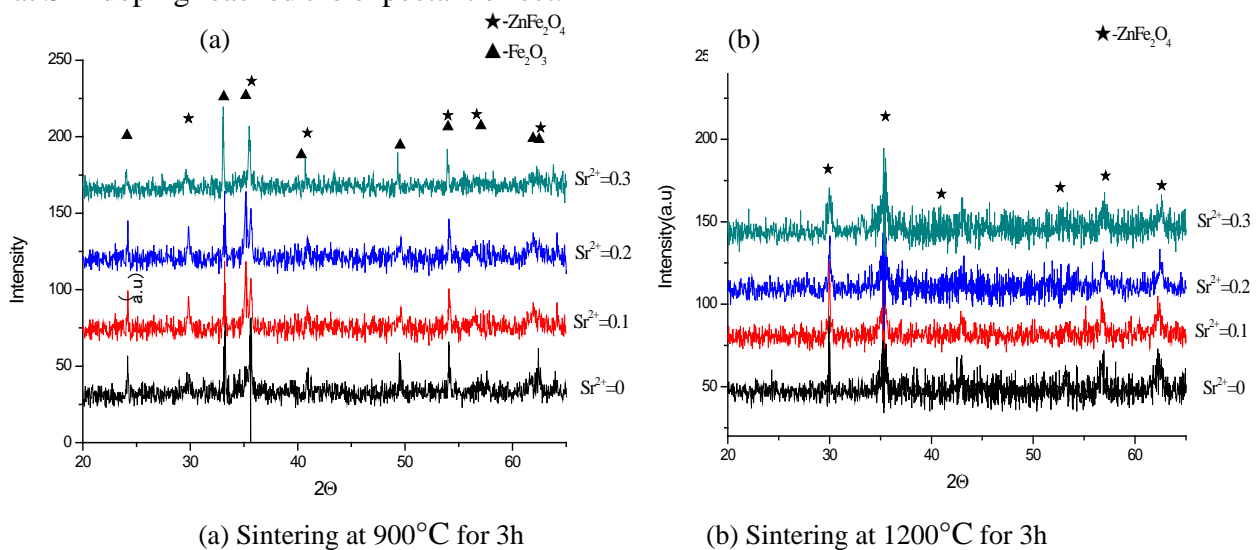
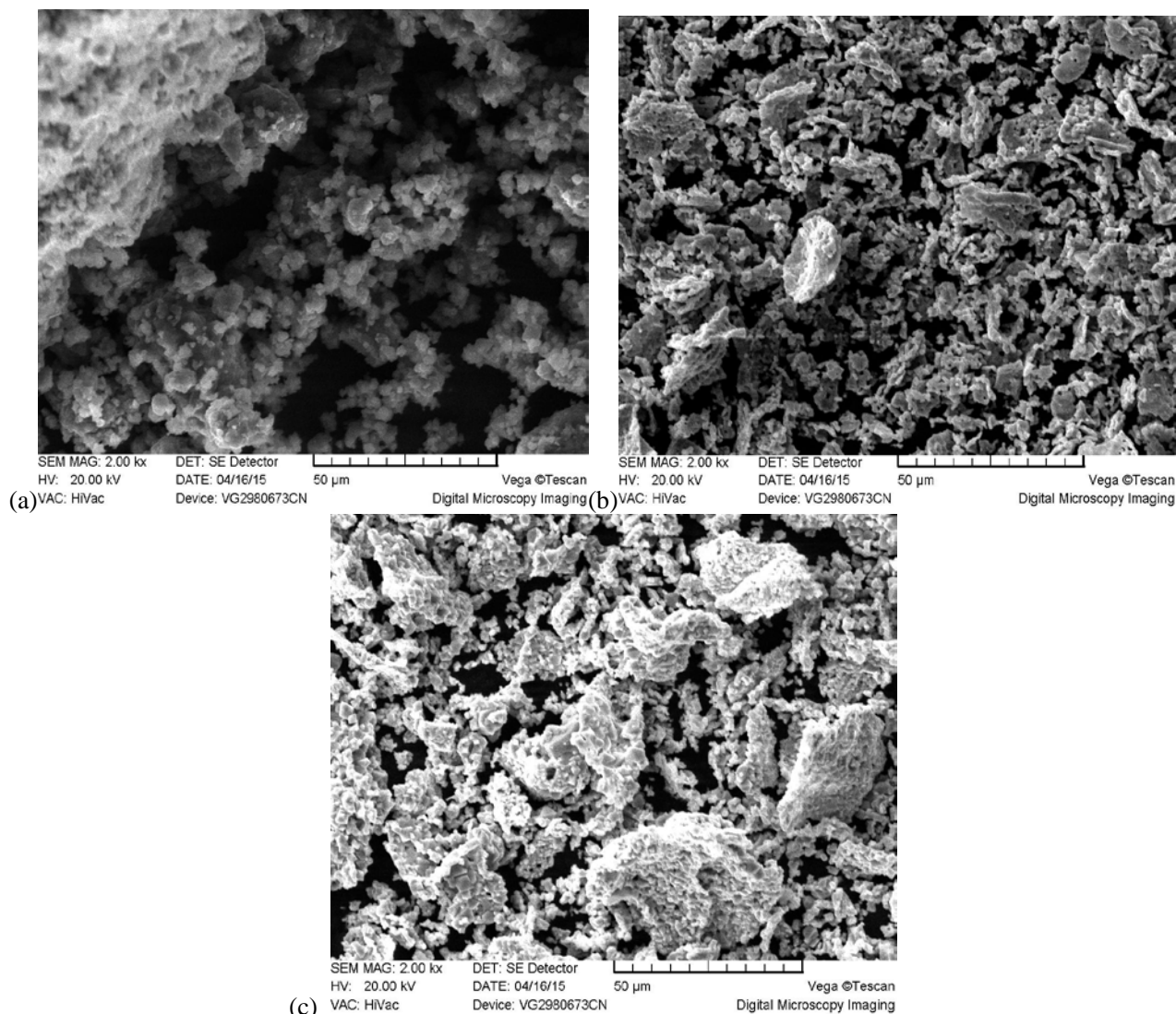


Figure 3.1 X ray spectrum by sintering at different temperature and different contents of  $\text{Sr}^{2+}$  doping

### Morphologies Observation

Morphologies of SEM were observed which were the precursor of 0.1% mol  $\text{Sr}^{2+}$  doping at low temperature self-propagating combustion, sintering for 3h at  $900^\circ\text{C}$  and sintering for 3h at  $1200^\circ\text{C}$  (see Figure 3.2(a),(b),(c)). It could be seen that morphology was closely link of honeycomb, fluffy and porosity after low temperature self-propagating combustion from the Figure 3.2(a). It was due to the precursor involved in a large amount of gas in the combustion process. Powder particle size was very small, and the nanometer particles were seen. After sintering at  $900^\circ\text{C}$  for 3h, the gas was expelled, reunion phenomenon of the powder was showed that most of the crystal grain size was larger, the phenomenon of secondary growth appeared, but there were still honeycomb pores, the uniformity of the grain size was poor(see Figure 3.2(b)). After sintering at  $1200^\circ\text{C}$  for 3h, powder inactivity increased further because of the increase of sintering temperature. Crystal grain became more coarse, reunion phenomenon was more obvious significantly(see Figure 3.2(c)).



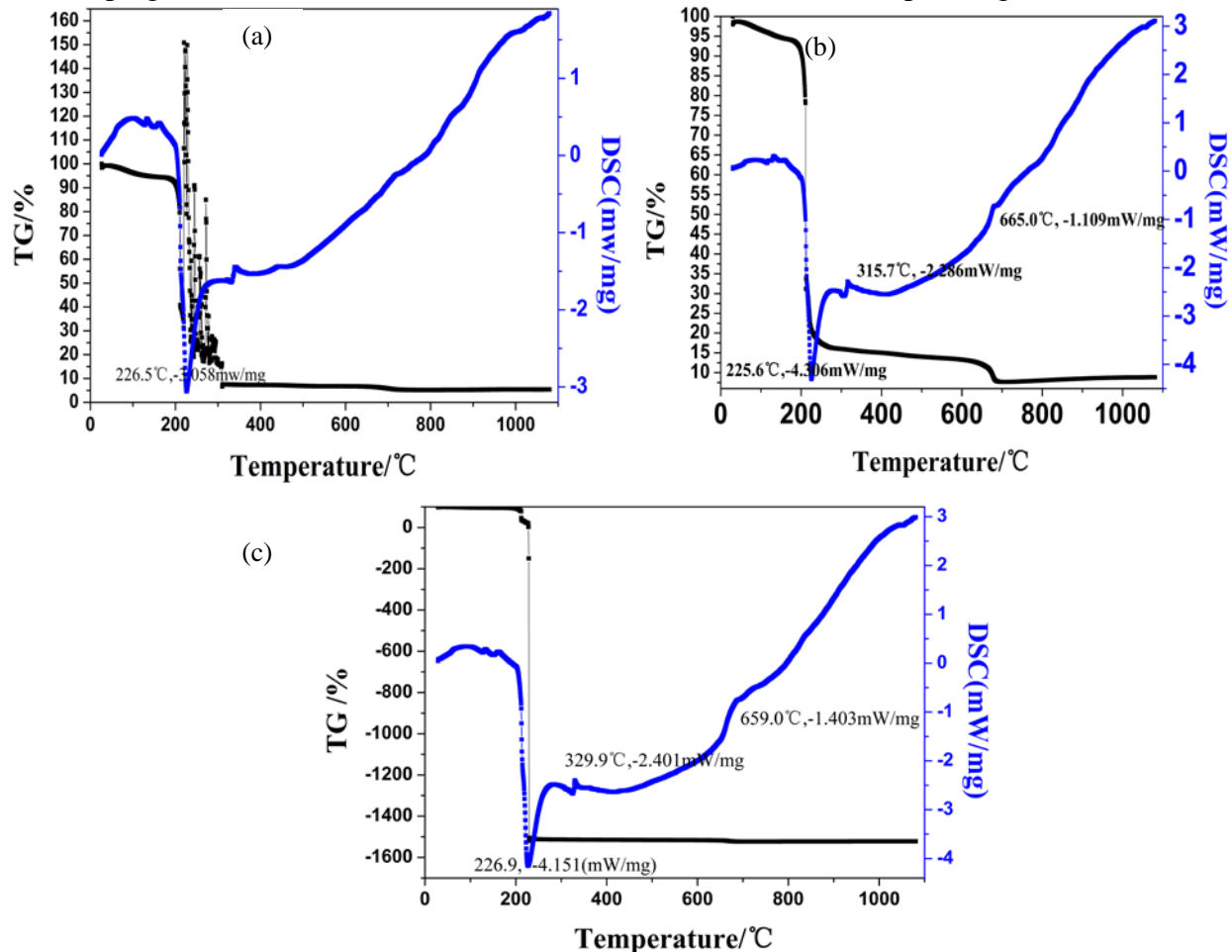
(a) Self-propagating combustion of the precursor at room temperature;  
 (b) Sintering at 900°C for 3h; (c) Sintering at 1200°C for 3h;

Figure 3.2 Morphologies of SEM for the precursor of 0.1mol%  $\text{Sr}^{2+}$  doping at different temperature

### TGA ( Thermogravimetric Analysis )

Different precursors of  $\text{Sr}^{2+}$  doping of DSC-TGA charts were showed in Figure 3.3. No  $\text{Sr}^{2+}$  doping was showed in Figure 3.3(a),  $\text{Sr}^{2+}$  doping (equal to 0.1mol%) was showed in Figure 3.3(b) and  $\text{Sr}^{2+}$  doping (equal to 0.2mol%) was showed in Figure 3.3(c). The abnormal fluctuations began to appear at about 200°C( see Figure 3.3(a)). It showed that a violent explosion happened. Dramatic REDOX reaction of nitrate ion and citrate polymer made nitrogen and nitrogen bond ruptured and carbonyl functional groups participate in the reaction. And then some kinds of gas including carbon dioxide, nitric oxide, water vapor and carbon monoxide released. Fluffy nano state of powder appeared because of a large number of gases. Reactions occurred very quickly, so the balance could not be synchronized in a moment, which led to abnormal readings. The similar phenomenon came forth in Figure 3.3(b) and Figure 3.3(c). An exothermic peak appeared in Figure 3.3(a) and three exothermic peaks appeared in Figure 3.3(b) and Figure 3.3(c). It could be seen that the first exothermic peak was around 227 °C when the reaction temperature began to appear from the three figures. Liberated heat was between 3mW/mg and 4mW/mg. Both reaction completed at near 650°C in Figure 3.3(a) and Figure 3.3 (b), while reaction completed at near 350°C in Figure 3.3(c), liberated heat was about 2.5mW/mg, which showed that the reaction became very significant and the reaction time became greatly shorten when the content of  $\text{Sr}^{2+}$

doping reached 0.2mol%. The reaction time was 130 seconds in Figure 3.3(a) and Figure 3.3 (b), lost weight reached more than 90% in this period, which meant that citric acid was consumed. The reaction time was only 15 seconds in Figure 3.3(c), the second exothermic peak appeared at near 330°C. A new phase probably generated due to  $\text{Sr}^{2+}$  doping. The third exothermic peak appeared at about 665°C, 1.109mW/mg of heat was liberated correspondingly(see Figure 3.3(b)), while at about 665°C and 1.403mW/mg (see Figure 3.3(c)). The reason probably was that  $\text{Sr}^{2+}$  ions entered octahedral crystal lattice, another new phase appeared respectively. With the increasement of the doping content, the reaction became more violent, and more new phases generated.



(a)  $\text{Sr}^{2+}=0\text{mol}\%$ , (b)  $\text{Sr}^{2+}=0.1\text{mol}\%$ , (c)  $\text{Sr}^{2+}=0.2\text{mol}\%$

Figure 3.3 DSC-TGA charts of Precursor for different content of  $\text{Sr}^{2+}$  doping

## Conclusions

1) The different concentration of  $\text{Sr}^{2+}$  doping on the synthesis of Mn-Zn ferrite precursor by sol-gel method was prepared. The final product was the  $\alpha\text{-Fe}_2\text{O}_3$  of paramagnetic impurity phase and the magnetic products  $\text{ZnFe}_2\text{O}_4$  of spinel phase at 900°C for 3h. The impurity disappeared when the sintering temperature arrived to 1200°C for 3h, and almost the entire  $\text{ZnFe}_2\text{O}_4$  phase was obtained. With the increasing concentration of  $\text{Sr}^{2+}$  doping, the main crystal surface (311) of  $\text{ZnFe}_2\text{O}_4$  has a small angle offset.

2) The Mn-Zn ferrite began to reunion when the sintering temperature arrived to 900°C. The most of crystal's grain was large, and the secondary growth phenomenon happened. But it still have the stomatal honeycomb. The size of grain's uniformity was poor. When the temperature arrived to 1200°C, the phenomenon of union was more obviously. Some grains even become to a large area, it grains become thicker.

3) The DSC-TGA charts of different concentration of  $\text{Sr}^{2+}$  doping on the synthesis of Mn-Zn ferrite precursor showed that a large number of moisture and so many inorganic such as citric acid

disappeared. The reason of this phenomenon was that it had a severe reaction because of self-propagating combustion when the temperature arrived to 226°C. As the increasing concentration of Sr<sup>2+</sup> doping, the reaction time reduced obviously, and the number of new phases became more than before.

## Acknowledgements

This work was financially supported by the Innovation and Entrepreneurship Training Program of College Students of Sichuan Province(project number: 201311360011).

## Reference

- [1] Yao Li-hua. The Mn-Zn ferrite present situation and development prospects in our country[J]. Advanced Materials Industry. Vol.9(2004):p.41-p.44.
- [2] He Shui-xiao. The future development trend of the manganese zinc ferrite materials[J].Journal of Magnetic Materials and Devices. Vol.6(2001):p.27-p.30.
- [3] FanYa-zhuo, Xu Qi-ming.The influence of addition on the microstructure and properties of Mn-Zn ferrites with high permeability[J].New Chemical Materials.Vol.34(2006):p.55-p.58.
- [4] Song Jie, Xu Nai-cen, Wang Li-xi etc.Sm<sup>3+</sup> doped a flect Mn-Zn ferrite microstructure and performance[J].Electronic parts and materials.Vol.9(2009):p.54-p.57.
- [5] Lan Zhong-wen, Zhang Yi-dong,Li Jin ect. Self-propagating high temperature synthesis technique preparation of Mn-power of znic ferrite[J].Journal of Magnetic Materials and Devices.Vol.1(2004):p.26-p.27.
- [6] Yue Zhen-xing, Zhou Ji, Zhang Hong-guo, ect. Self combustion of citric acid salt gel and synthesis of iron oxide nanoparticles[J].Journal of silicate. Vol.4(1999):p.466-p.470.
- [7] Luo Guang-shen, Li Jian-de ect. Process and Structure Research on Preparation of Mn-Zn ferrite by Coprecipitation and oxides methods[J]. Journal of Nan Chang Univesity. Vol.4(2009):p.34-p.38.
- [8] Yan Shi-feng. Preparation of Magnetic Nanocomposites and the Study of the Magnetic Properties[D]. ChangChun: ChangChun Institute of Applied Chemistry Chinese Academy of Sciences. 2005.
- [9] Li Bo-gang,Yi Guang-fu,Han Ji-mei ect. Analysis of the thermodynarnic conditions for the coprecipitation conditions of the preparation of soft manganese ferrite power[J].Rare Metals.Vol.6(1996):p.22-p.25.
- [10] Zhang Mi-lin. Citri acid synthesis SrFe<sub>12</sub>O<sub>19</sub> super powder[J]. Journal of silicate, Vol.6(1996):p.685-p.688.
- [11] Zhao Jian-du, Liang Yong-qing, Yan Hong-jun ect. Nano scale Mn-Zn ferrite prepared by dry gel method[J].Materials Science and Engineering. Vol.1(2003):p.68-p.71.
- [12] Zhu Sheng-Chuan, Chen Hai-ying. Research on the magnetic spectrum of power-supply ferrite[J]. Journal of Maganetism and Maganetic Materials, Vol.181(1998):p.259-p.264.
- [13] Yu Zhong, Lan Zhong-wen, Wang Jin-mei etc. Preparation of MnZn Ferrite Powders by Sol-Gel Process [J]. Journal of functional materials, Vol.4(2000):p.484-p.487.